Evaluation of a Pumping Assist Lung That Uses a Rotating Fiber Bundle

Robert G. Svitek,*† Brian J. Frankowski,* and William J. Federspiel,*†‡§

A paracorporeal respiratory assist lung (PRAL) is being developed for supplemental gas exchange to allow the native lungs of acute lung failure patients to heal. The device consists of a rotating annular microporous hollow fiber membrane bundle. The rotation augments the gas exchange efficiency of the device at constant flow-rate thereby uncoupling gas exchange and flow rate. The rotating fibers also enable the PRAL to pump the blood without the need for an additional pump or arterial cannulation. Blood flow rates will be between 500 and 750 ml/min with CO_2 removal rates of 100–130 ml/min. A prototype was manufactured with an overall surface area of 0.25 m^2. When rotated at 1500 rpm, CO_2 removal increased by 133% and O_2 transfer increased by 157% during an *in vitro* bovine blood study. The pumping of the rotating fiber bundle was assessed in a glycerol/water solution. At 1500 rpm, the PRAL generated 750 ml/min against 52 mm Hg pressure. Hemolysis of the device was assessed using *in vitro* bovine blood from a slaughterhouse. Plasma free hemoglobin levels were similar regardless of whether the rotating fibers were present in the PRAL, indicating that a rotating fiber bundle can be used to increase gas exchange without causing blood trauma. *ASAIO Journal* 2005; 51:773–780.

Lung disease is the number three killer in America and is responsible for nearly 350,000 deaths every year.[1] Acute respiratory distress syndrome (ARDS) is an acute lung disease associated with pneumonia, shock, sepsis, or trauma. The disease affects 150,000 Americans each year,[2] and the mortality rate is approximately 50% for anyone diagnosed with ARDS.[3] Chronic obstructive pulmonary disease (COPD) is another lung disease characterized by airflow obstruction, dyspnea, and increased blood CO_2 content and affects approximately 4–10% of adults.[4] Acute exacerbations of ARDS and COPD may be reversible if the lungs can be temporarily supported and allowed to heal.[5–9] Current treatment protocols, however, implement mechanical ventilation that forces oxygen into and out of the lungs at pressures and volumes that may cause further damage to the lungs.[6,10] Unfortunately, the end result of this treatment has been high mortality and morbidity in patients with acute lung failure such as ARDS and COPD.[11–13]

In the late 1970s, Kolobow and Gattinoni suggested extracorporeal CO_2 removal as a means for supplemental gas exchange to reduce ventilator settings allowing the natural lungs to rest.[14–20] The concept consisted of taking blood outside of the patient with a pump, removing CO_2 with a membrane oxygenator, and pumping the blood back to the patient. Extracorporeal CO_2 removal has since evolved into a simpler system known as arteriovenous CO_2 removal (AVCO2R).[21] Blood flows from an arterial femoral cannulation to a blood oxygenator and then back to the venous system of the patient through a femoral return cannula, thus eliminating the need for a pump. AVCO2R has been shown to achieve significant CO_2 removal at lower blood flow rates than typically used in extracorporeal membrane oxygenation.[21–23] The blood flow rate in AVCO2R systems depends on a combination of the arterial-venous pressure gradient of the patient and the resistance of the blood oxygenator and cannula. Studies of AVCO2R have been performed in animal models of ARDS, and have expanded into human clinical trials. Mechanical ventilation parameters such as tidal volume, minute ventilation, and peak pressure were reduced as a direct result of the low flow CO_2 removal of AVCO2R.[22,24]

We are developing a paracorporeal respiratory assist lung (PRAL) that targets clinically significant CO_2 removal at a low blood flow rate. A schematic representation of the PRAL is shown in **Figure 1**. Percutaneous cannula (either one dual lumen or two single-lumen cannula) will be inserted through the femoral vein into the vena cava for blood flow to and from the PRAL. The PRAL uses an annular rotating hollow fiber membrane bundle to increase gas exchange efficiency through active mixing of the blood around the fibers, which ultimately uncouples gas exchange and blood flow rate. Typical passive oxygenators used in cardiopulmonary bypass depend on increased flow rate to achieve higher levels of gas exchange, whereas with the PRAL, gas exchange can be augmented by increasing the fiber bundle rotation rate while maintaining a constant low flow rate. The increase in gas exchange efficiency due to rotation also enables a lower membrane surface area than commercially available membrane oxygenators. The reduction in surface area may lead to decreased platelet activation and reduced thrombosis.[25] Additionally, the rotating fiber bundle generates pumping pressure which enables veno-venous circulation without the need for an arterial cannulation. Venous cannulation may reduce the inherent blood loss and bleeding risks associated with arterial cannulation. The

From the *McGowan Institute for Regenerative Medicine, Departments of †Chemical Engineering, ‡Surgery, and §Bioengineering, University of Pittsburgh, Pittsburgh, PA.

Submitted for consideration May 2005, accepted in revised form July 2005.

Reprint Requests: William J. Federspiel, PhD, University of Pittsburgh, 215 McGowan Institute for Regenerative Medicine, 3025 East Carson St., Pittsburgh, PA 15203; E-mail: federspielwj@upmc.edu

DOI: 10.1097/01.mat.0000178970.00971.43

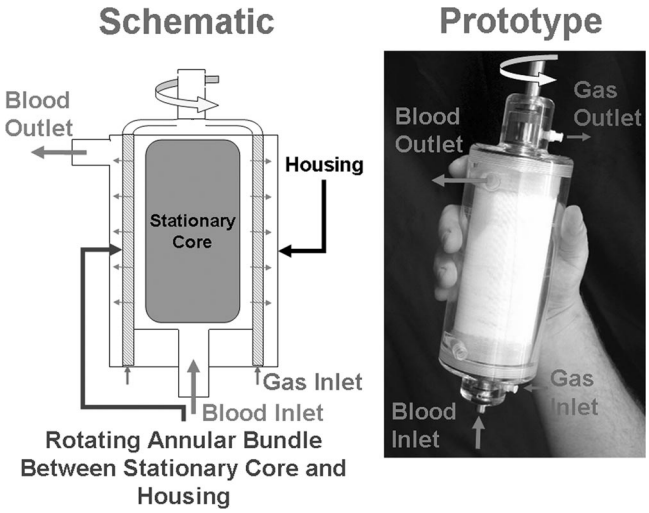

Figure 1. Schematic of patient connected to PRAL. A single dual-lumen cannula provides blood flow to the device from the patient and vice-versa. The rotating fiber bundle within the device provides enhanced gas exchange and pumping.

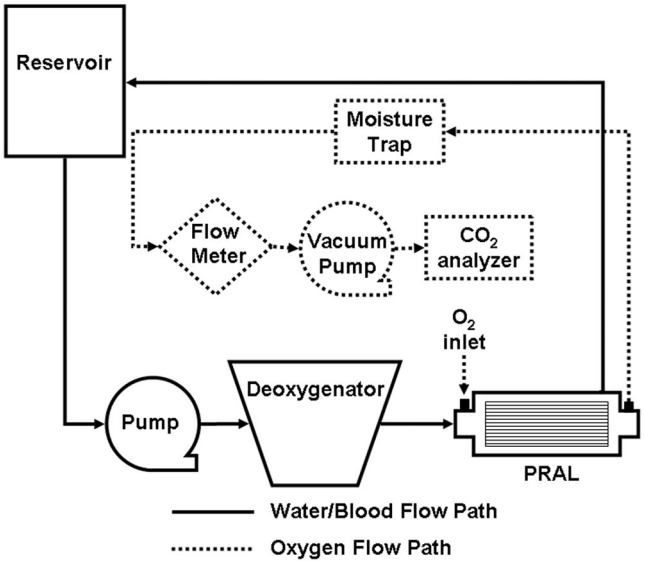

Figure 2. Mock loop for testing the gas-transfer ability of the PRAL.

target CO_2 removal for the PRAL is 100–130 ml/min at blood flow rates from 500–750 ml/min to reduce ventilator settings and allow the native lungs of the patient to heal. Duration of support is targeted for 7–10 days for patients with acute respiratory failure.

The concept of using rotation in a membrane oxygenator has been around for some time. Several investigators in the 1970s used rotation to increase gas exchange in artificial lungs made from flat microporous membrane sheets.[26–28] These devices were large in size because of the inherently low surface area/volume ratio of membrane sheets. Other investigators have attempted to use rotation in disk-shaped oxygenators that exhibited high hemolysis levels due to their complex construction and operation.[29–31] Makarawicz *et al.* manufactured and tested gas exchange and pumping in the pumping artificial lung (PAL) in the mid 1990s.[32,33] The PAL was manufactured using a modified viscous blood pump housing, and its intended use was for simplifying cardiopulmonary bypass. This prototype exhibited an increased pumping ability with rotation; however, gas exchange was not increased with rotation at constant flow rate. Development in the area of rotating hollow fiber membrane bundles has since been sparse.

In this study, we investigate the feasibility of the PRAL concept using an initial prototype device. The principal goals of the study are 1) to measure the gas exchange performance of the initial PRAL prototype in water and blood; 2) to show that gas exchange can be significantly enhanced by rotation of the fiber bundle; 3) to show that the rotating bundle of the PRAL prototype allows the device to pump blood appropriate to its intended application; and 4) to demonstrate that blood damage (hemolysis) caused by the means by which gas exchange is enhanced and the device pumps, *i.e.*, the rotation of the fibers within the bundle of the PRAL, is not significant.

Materials and Methods

Prototype Description

The initial PRAL prototype studied here was fabricated with a gas exchange surface area of 0.25 m^2 composed of uncoated microporous polypropylene fibers with an outer diameter of 300 μm and an inner diameter of 240 μm (Celgard, ARX30240, Charlotte NC). The fiber bundle had a thickness of five layers of fibers, a length of 13 cm, and an overall diameter of 6.6 cm. The fibers were wrapped and potted to a stainless steel support structure that coupled to the motor drive shaft. The support structure eliminated torque applied directly to the fibers during bundle rotation. The stationary center core was fabricated from clear acrylic, and four holes were machined at the upstream end of the core for blood to enter into the fiber bundle. The gaps between the fiber bundle and the stationary walls on the inner and outer sides of the bundle were 4 mm and 2 mm, respectively. The housing that surrounded the fiber bundle was made from a stock piece of clear acrylic and consisted of three components, two endcaps, and a center piece that contained the outlet port. The blood inlet was located in the upstream endcap and connected to the center core for blood to enter the fiber bundle. Gas entered and exited the device through side ports in the endcaps and flowed through the lumens of the fibers. The gas pathway was separated from the blood pathway by 3/8″ ID nitrile seals (CRseals, 6119, Elgin, IL). A stainless steel shaft connected the fiber bundle to the drive motor through the distal endcap.

In Vitro Gas Exchange

The gas exchange of the PRAL prototype was characterized in water and bovine blood from a local slaughterhouse. The blood was filtered with 40 μm pore size filters (Pall Biomedical, SQ40S, Fajardo PR) on the day of collection to remove any hair or extraneous particles due to the collection process, and Gentamicin (0.1 g/mL) was added to prevent infection. A flow loop was constructed for both water and blood testing that consisted of a reservoir, a centrifugal pump (March Manufacturing, LC-2CP-MD, Glenview IL), a commercial oxygenator (Affinity, Medtronic MN), and the PRAL prototype (**Figure 2**). Tubing connected the outflow port of the reservoir to the inlet of the centrifugal pump. The pump was used in conjunction

with a Hoffman clamp to set the flow rate to 750 ml/min. Sweep gas through the commercial oxygenator was a N_2/CO_2 mix adjusted with a gas blender (Cole-Parmer Instrument Company, PMM2-010032, Vernon Hills, IL) to set the inlet conditions in accordance with the Association for the Advancement of Medical Devices standards[34]: O_2 inlet saturation 65 ± 5% and inlet pCO_2 of 45 ± 5 mm Hg. The test fluid flowed from the commercial oxygenator into the PRAL and then back to the reservoir. The flow rate was measured using a flow probe (Transonic Systems, Inc, T110, Ithaca, NY). O_2 partial pressures at the inlet and outlet of the device were measured using a blood-gas analyzer (ABL-505 Radiometer Copenhagen, Denmark). The concentration and saturation of hemoglobin was measured with an OSM3 Hemoximeter (Radiometer). Pure oxygen sweep gas flowed under vacuum through the PRAL fiber lumens at 6.5 l/min. The gas then flowed through a moisture trap and through a Top Trak flow meter (Sierra Instruments, 822-13-OV1 PV1-V1, Monterey CA). A vacuum pump (Barnant, 400-3910, Barrington, IL) and needle valve were used to maintain constant sweep gas flow through the device. A CO_2 analyzer (Physiodyne, CO2-44B, Quogue, NY) was used to measure the concentration of CO_2 exiting the gas stream of the PRAL. Oxygen transfer rates in blood (V_{O_2}) were calculated using the following relationship [35]:

$$V_{O_2} Q[\, a_{O_2} P_{O_2}^{\text{out}} - P_{O_2}^{\text{in}}) + C_T \Delta S] \tag{1}$$

where Q is the blood flow rate, a_{O_2} is the solubility of O_2 (3.16E-4 ml O_2/ml blood/cmHg), and ($P_{O_2}^{\text{out}} - P_{O_2}^{\text{in}}$)is the difference in partial pressure between the inlet and outlet of the device. C_T is the hemoglobin binding capacity of blood (0.167 ml O_2/ml blood), and ΔS is the change in saturation of the hemoglobin from the inlet to the outlet. O_2 transfer in water was calculated by setting ΔS equal to zero in Equation 1 and using a solubility of 3.0E-4 ml O_2/ml H_2O/cmHg.[36]

Carbon dioxide removal rate (V_{CO_2}) was calculated from the sweep gas flow rate (Q_{OUT}^{STP}) and CO_2 fraction (F_{CO_2}) exiting the PRAL:

$$V_{CO_2} = Q_{OUT}^{STP} F_{CO_2} \tag{2}$$

Variations in the inlet pCO_2 can affect the overall gas exchange of the device. For example, an inlet pCO_2 of 45 mm Hg will have a lower CO_2 removal rate than an inlet pCO_2 of 50 mm Hg because this 5 mm Hg difference in inlet conditions corresponds to a 10% difference in concentration gradient across the fiber membranes. Therefore, the CO_2 exchange was normalized to an inlet pCO_2 of 45 mm Hg to reduce the variability associated with fluctuating inlet conditions [37]:

$$V_{CO_2}^{*} = V_{CO_2} \frac{45}{pCO_2^{\text{INLET}}} \tag{3}$$

If the inlet value differed by more than 45 ± 5 mm Hg, the inlet concentration was adjusted by changing the sweep gas through the commercial oxygenator and the sample was taken again.

In Vitro Pumping in Blood Analogue Fluid

The pumping ability of the PRAL was quantified in a recirculating flow loop with a reservoir, the PRAL, and 3/8″ laboratory tubing (**Figure 3**). Pumping at rotation rates of 1500 and 1000 rpm was evaluated. The test fluid was a blood analogue consisting of a 2:3 part mixture of glycerol to water by volume with a viscosity of 3.4 cP measured with a falling ball viscometer (Gilmont Instruments, GV-2100, Barrington IL). The flow rate of the fluid was measured with the Transonic flow probe and the pressure difference across the device was measured using a differential pressure transducer (Validyne Engineering Corporation, CD379, Northridge, CA). At constant speed (rpm), the flow rate was throttled down incrementally to zero flow (shut off head) using a Hoffman clamp. At each flow rate, the pressure increase across the device was measured.

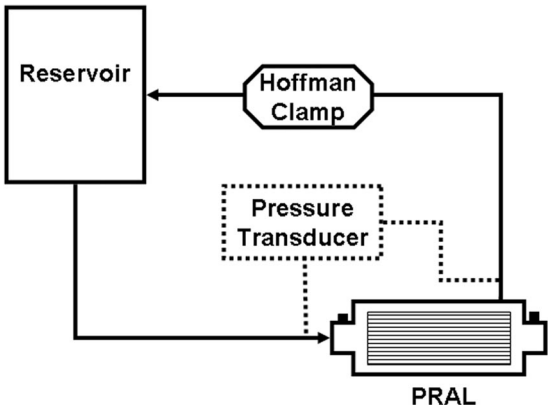

Figure 3. Mock loop for testing pumping ability of the PRAL.

In Vitro Hemolysis

Hemolysis tests were conducted on the PRAL to assess the blood damage caused by rotating the fiber bundle. The experimental setup consisted of two identical test loops: one for evaluation of hemolysis of the PRAL and one for evaluation of hemolysis of a control oxygenator, the Capiox (Terumo, Capiox, Japan). Each loop contained a blood reservoir, a heat exchanger, a Biomedicus pump, the test device, and 3/8″ Tygon laboratory (formulation R3603) tubing connecting the components together. The priming volume of each loop was 1.5 L. The fiber bundle was rotated at 1000 rpm, and the flow rate was adjusted with the Biomedicus pump to 750 ml/min. Blood was added to the control loop within 30 minutes and this loop was circulated until the temperature reached 37ºC. Samples (4 ml) were drawn from each loop every half hour for the first 2 hours and every hour thereafter for the duration of the 6-hour evaluation. Each sample was used to measure hematocrit and plasma free hemoglobin (PfHB). Hematocrit was measured with a capillary tube spun down for 3 minutes in a microhematocrit centrifuge (International Equipment Co., IEC MB, Needham Hts, MA). The remainder of the sample was spun down in a centrifuge at 3400 rpm for 15 minutes. The supernatant plasma was siphoned off into an Eppendorf tube and spun down again at 10000 rpm for another 15 minutes. The purified plasma was transferred to a cuvette and analyzed in a spectrophotometer (Thermo Spectronic Genesys 5) at a wavelength of 540 nm. The absorption of light by the spectrophotometer was calibrated to known levels of PfHB.

Plasma free hemoglobin levels were measured over time in a recirculating loop for the PRAL and then the same test was

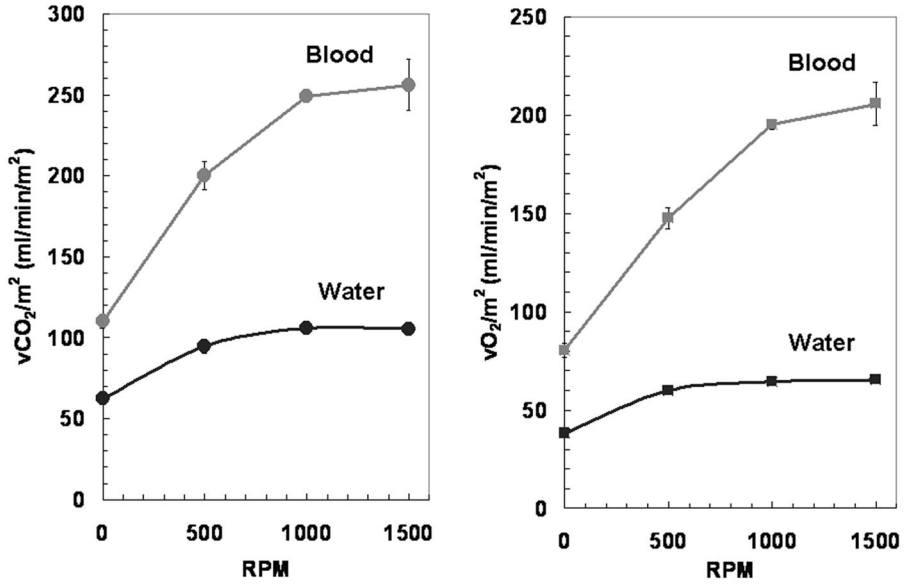

Figure 4. Gas exchange results for PRAL in water and blood as a function of fiber bundle rotation rate. The flow rate was constant at 750 ml/min.

repeated with a different batch of blood on a different day after removing the PRAL fibers. A control oxygenator was tested simultaneously during each of these tests to compare differences between batches of blood. Blood damage was expressed as a Normalized Index of Hemolysis (NIH) according to the following equation[38]:

$$\mathrm{NIH} = \frac{\Delta \mathrm{PfHb} \cdot V \cdot 1 - \mathrm{HCT}/100 \cdot 100}{\Delta t \cdot Q}$$

where $\Delta PfHb$ is the change in plasma free hemoglobin levels, V is the priming volume of the circuit, HCT is the hematocrit of the blood sample, Q is the flow rate of blood, and Δt is the time duration of the test.

Results

The gas exchange of the PRAL in water and blood is shown in **Figure 4** as a function of rotation rate. In water, the PRAL prototype shows enhancement with increasing rotation rate at constant flow rate and the CO_2 removal per fiber bundle surface area increased from 62 ± 2 ml/min/m^2 to 106 ± 3 ml/min/m^2 over the range of 0 to 1500 rpm. The O_2 supplied to the water also increased with rotation from 38 ± 1 to 65 ± 1 ml/min/m^2 over the range of 0 to 1500 rpm. For both CO_2 and O_2 exchange in water, these increases correspond to over 70% increase in gas exchange due to the rotation of the fiber bundle. In blood, the CO_2 removal per fiber bundle surface area was 110 ± 4 ml/min/m^2 at 0 rpm and increased to 256 ± 16 ml/min/m^2 at 1500 rpm. The O_2 supplied per fiber bundle surface area increased from 80 ± 4 ml/min/m^2 to 206 ± 11 ml/min/m^2. Maximum overall gas exchange occurred at 1500 rpm with 64 ± 4 ml/min of CO_2 removed and 52 ± 3 ml/min of O_2 supplied.

The pump curves for the PRAL prototype in a glycerol/water

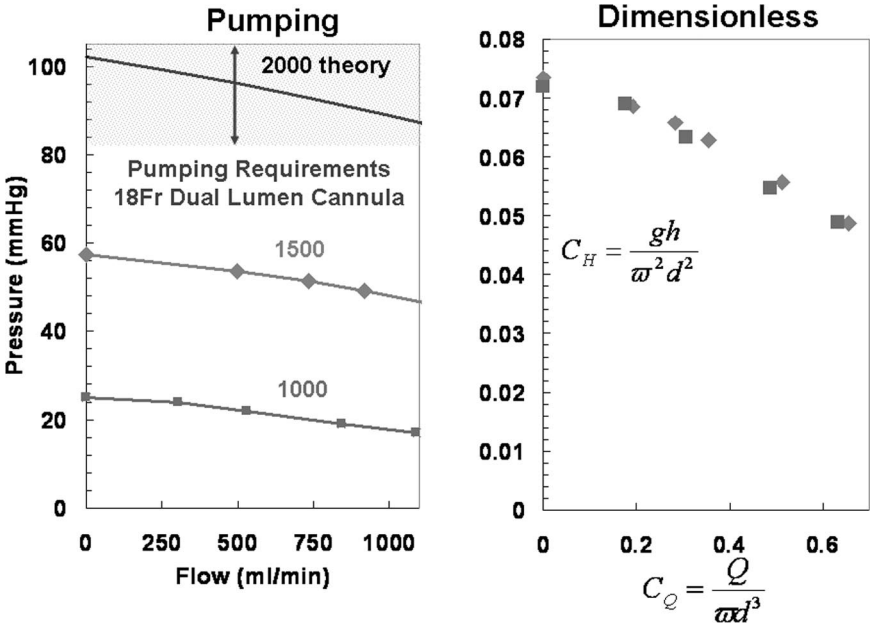

Figure 5. A: Pump curves of PRAL at rpm of 1000 and 1500 in a water/glycerol solution with a viscosity of 3.4 cP. The system curve is also plotted to estimate the clinical performance criteria for the PRAL. B: Dimensionless pump curves of PRAL that can be used to estimate the pumping ability at any rotation rate.

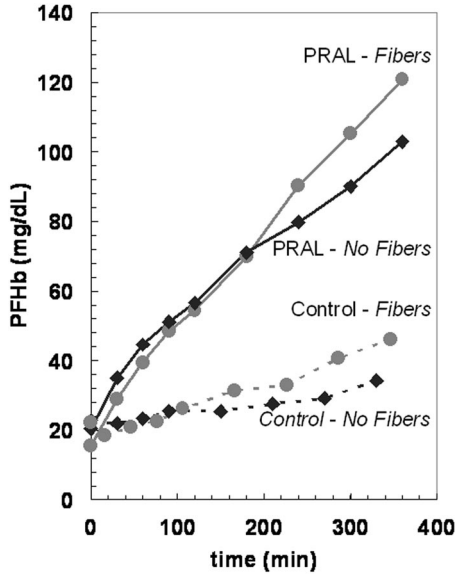

Figure 6. Plasma free hemoglobin concentration during fiber bundle rotation of 1000 rpm with and without the fibers in the device. The increase in plasma free hemoglobin is similar for both cases.

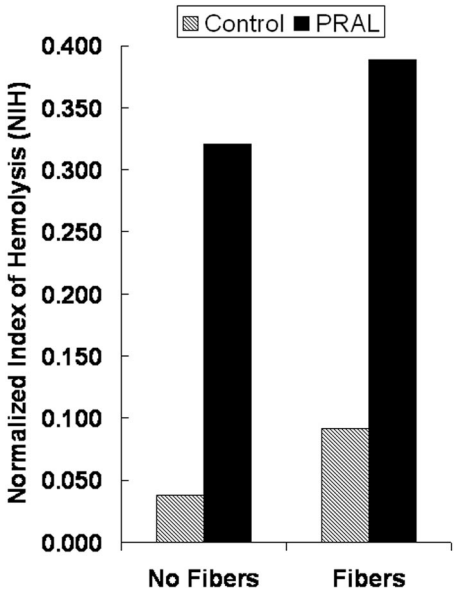

Figure 7. Normalized Index of Hemolysis (NIH) for the PRAL with and without fibers and the corresponding NIH for the control loops.

solution are shown in **Figure 5a** up to a flow rate of 1000 ml/min. The pressure generated by the rotating fiber bundle at 1500 rpm ranged from 57 mm Hg at no flow (shut off head) to 51 mm Hg at 734 ml/min. At 1000 rpm, the pressure ranged from 25 mm Hg at no flow to PRAL generated 22 mm Hg at 530 ml/min.

The hemolysis results are shown in **Figure 6** for the PRAL device and the PRAL device with the fibers removed. Also shown on the graph are the PfHB levels for the corresponding control loops that were tested at the same time as the PRAL with and without fibers. The PfHB level for the PRAL increased from 15.6 to 120.8 mg/dL, and the PfHB level in the control loop tested on the same day with the same blood increased from 22.1 to 46.1 mg/dL. The PfHB level in the loop containing the PRAL device with the fibers removed increased from 20.4 to 102.9 mg/dL and the PfHB level in the Terumo control loop tested on the same day with the same batch of blood as the PRAL without the fibers increased from 22.9 to 33.6 mg/dL. The NIH values for the two experiments are shown in **Figure 7**. The NIH was 0.389 for the PRAL and 0.091 for the control. For the PRAL without fibers, the NIH was 0.321 and 0.038 for the corresponding control loop.

Discussion

Mechanical ventilation is the current treatment for acute exacerbations of lung diseases such as ARDS and COPD, but mortality and morbidity remain high due to ventilator induced trauma. We are developing a paracorporeal PRAL to aid the breathing of the patient to enable the native lungs to heal. The gas exchange of the assist lung will allow reduced ventilator settings or possibly complete weaning from the ventilator altogether. Our assist lung uses a rotating hollow fiber membrane bundle for increased gas exchange and self-pumping. We tested the feasibility of this design by building a prototype and measuring gas exchange in water and blood and measuring the pumping ability in a glycerol-water blood analogue. We also evaluated the hemolysis of the PRAL *in vitro* using slaughterhouse bovine blood. Gas exchange in the PRAL increased with increasing rotating rate of the bundle at constant flow rate through the device. In blood, CO_2 removal increased 133% and O_2 supplied increased 158% at 1500 rpm over the stationary bundle. In addition to enhanced gas exchange, the PRAL pumped 750 ml/min of flow against a pressure of 52 mm Hg. In a series of *in vitro* hemolysis tests of the PRAL, the increase in plasma-free hemoglobin over time was not due to the rotating fibers within the bundle.

Achieving adequate gas exchange at blood flow rates 750 ml/min or less requires either a large membrane surface area, or a high gas exchange per membrane area. The Affinity artificial lung that is used in AVCO2R is passive and achieves approximately 50 ml/min/m^2 of CO_2 removal efficiency at a blood flow rate of 1 l/min.[39] This level of efficiency requires a surface area in excess of 2 m^2 to achieve 100 ml/min of CO_2 removal. By contrast the rotation of the fiber bundle in the PRAL generates CO_2 removal efficiency of 250 ml/min/m^2 at 1500 rpm. The increase in efficiency enables a smaller membrane surface area than a passive artificial lung. The PRAL prototype described in this study was fabricated with a surface area of 0.25 m^2 primarily to show feasibility of a rotating bundle to increase gas exchange and pump. If the fiber bundle can be designed such that CO_2 removal efficiency scales with surface area, then our current design would only require 0.4 m^2 surface area to achieve 100 ml/min of CO_2 removal.

We believe that the shear stress from the stationary walls surrounding the rotating fiber bundle is the mechanism behind gas exchange enhancement in the PRAL. The shear stress caused by the stationary walls penetrates into the bundle and opposes the drag force imparted by the rotating bundle on the blood. The relative velocity between the fibers and the blood is due to the shear stress within the bundle. As rotation rate is increased, the shear stress within the bundle increases, and

therefore relative velocity between the fibers and the blood also increases leading to gas exchange enhancement. We have tried to maximize this shear penetration by minimizing the distance between the stationary walls and the rotating fiber bundle to within several millimeters. Additionally, the rotating fiber bundle is only five fiber layers thick so that two of these layers are rotating directly adjacent to the stationary walls. We believe that as fiber bundle thickness is increased with more layers, the blood will become entrained in the rotating bundle leading to lower relative velocity within the bundle. Therefore, gas exchange enhancement will diminish as fiber bundle thickness increases. The absence of gas exchange enhancement of the PAL reported by Makarawicz *et al.*[32,33] may be due to the lack of a stationary center core in addition to the device having a thick fiber bundle compared with the PRAL fiber bundle.

The rotating fiber bundle generates pressure that enables the PRAL to pump. In this study, we tested the pumping ability in a glycerol/water solution with a kinematic viscosity similar to that of whole blood. Under the shear conditions in the PRAL, blood will act as a Newtonian fluid, so we believe that the glycerol/water mixture provides a realistic estimation of the performance of the PRAL in blood. We can estimate the pressure that the PRAL will need to generate from the pressure-flow relationship of a dual lumen cannula commonly used in pediatric ECMO (Origen Biomedical, REF). The cannula is 18 Fr and in the flow range of 500–750 ml/min the pressure drop ranges from 80–100 mm Hg. **Figure 5A** shows the current PRAL pumping ability with the estimated pressure drop of the proposed cannula (hatched region). The current PRAL prototype generated 52 mm Hg at 750 ml/min at 1500 rpm, approximately half of the required pumping ability. One way to increase the pumping ability is to increase the angular frequency of the rotating fiber bundle. We can estimate the rotation rate that will generate 80–100 mm Hg pressure by transforming the pump curves into two dimensionless groups, the head coefficient defined as $C_H = \frac{gh}{\varpi^2 d^2}$ and the flow coefficient defined as $C_Q = \frac{Q}{\varpi d^3}$ where g is the gravitational constant, h is the head generated by the pump, ω is the angular frequency of the fiber bundle, and d is the diameter of the fiber bundle. Transforming the data in this way collapses the pump curves into one universal curve **(Figure 5B)** that can be used to estimate the PRAL pumping ability at any angular frequency. The theoretical pumping ability at 2000 rpm is shown in **Figure 5A** as a solid line. At this angular frequency, the PRAL pump curve is within the pressure-flow characteristics of the cannula, indicating that this cannula can be used for our application.

The rotating fibers in the PRAL cause minimal damage to the red blood cells. NIH was 0.389 for the PRAL compared with 0.321 for the PRAL with the fibers removed representing a difference of 17%. However, the rate of PfHB increase for the control loop tested against the PRAL was 0.091 compared with 0.038 for the same control loop tested against the PRAL with the fibers removed, representing a difference of nearly 60%. The large disparity in the NIH values in the control loops suggests large differences in the fragility of the blood used on the different test days. The disparity in blood batches may explain any difference between the PRAL with and without fibers.

A simple shear stress analysis is further evidence that the rotating fibers do not cause blood damage in the PRAL. Hemolysis is a function of exposure time and shear stress, but is not problematic when blood elements are exposed to shear stresses < 1500 dynes/cm^2.[40] Maximum shear stress due to the rotating fiber bundle occurs at the surface of the outer layer of fibers. An order of magnitude estimation of this maximum shear stress is given by

$$\tau \cong \frac{\mu \omega R_0}{\varsigma_{gap}}$$

where μ is the viscosity of blood, ω is the angular frequency of the fiber bundle, R_o is the outer radius of the fiber bundle, and δ_{gap} is the gap thickness between the rotating fiber bundle and the outer stationary housing. Blood has a viscosity of 3 cP,[41] the outer radius of the fiber bundle is 3.3 cm, and the gap thickness is 0.2 cm. Therefore, the maximum shear stress due to rotation is on the order of 80 dynes/cm^2, or two orders of magnitude less than the threshold for red cell damage.[40] Our estimations of shear stress due to the rotating fiber bundle indicate that the rotating fiber bundle in the PRAL should not induce significant blood damage thus helping to validate our experimental result that the fibers are not the main source of hemolysis.

One possible cause for the current level of hemolysis in the PRAL may be the blood flow path within the device. The inflow and outflow ports could cause high shear recirculation zones that would lead to elevated hemolysis. Computational fluid dynamics (CFD) and flow visualization techniques have become useful tools in determining high shear regions in blood pumps.[42–48] We plan to analyze the PRAL using CFD and flow visualization to locate any potential zones of high shear and recirculation. Additional causes for elevated blood damage may be the seals and bearing used in the current prototype. Heat generation is a common problem in blood pumps that contain seals around a rotating shaft.[49,50] Infusion of heparinized saline around the rotating shaft can flush the area with fresh fluid to reduce heat and stagnation.[51] Seals made of ferromagnetic fluid are another solution that shown promise in minimizing blood damage.[50] Finally, a magnetic coupling could also be used to rotate the bundle to eliminate the seal and bearing altogether.[52]

Conclusion

Treating acute lung failures like the exacerbations of ARDS and COPD will require better outcomes than those achieved with mechanical ventilation. We are developing a PRAL with a rotating annular hollow fiber membrane bundle to temporarily supplement the gas exchange of the native lungs so they can heal. The PRAL demonstrates increased gas exchange with rotation, pumping ability, and minimal hemolysis caused by the rotation of the fibers. Implementing the PRAL will provide venovenous gas exchange at a low blood flow rate to reduce ventilator settings or weaning from the ventilator completely.

Acknowledgment:

This work was supported by the National Tissue Engineering Consortium (NTEC), the US Army Medical Research Acquisition Activity, 820 Chandler Street, Fort Detrick, MD 21702-5014, grant number DAMD17-02-0717. The publication was also made possible by grant RO1 HL70051 from the National Institutes of Health, the National

Heart, Lung, and Blood Institute. Its contents are solely the responsibility of the authors and do not necessarily represent the official views of any of the mentioned sources of funding. The authors acknowledge the support of the University of Pittsburgh's McGowan Institute for Regenerative Medicine.

References

1. Data and statistics. Available at: http://www.lungusa.org/site/pp.asp?c=dvLUK9O0E&b=33347. American Lung Association. 2004. Accessed February 2005.
2. Demling RH: The modern version of adult respiratory distress syndrome. *Ann Rev Med* 46: 193–202, 1995.
3. Zilberberg MAD, Epstein SK: Acute lung injury in the medical ICU: Co-morbid conditions, age, etiology, and hospital outcome. *Am J Respir Crit Care Med* 157: 1159–1164, 1998.
4. Halbert RJ, Isonaka S, George D, Iqbal A: Interpreting COPD prevalence estimates: what is the true burden of disease? *Chest* 123: 1684–1692, 2003.
5. Hirvela ER: Advances in the management of acute respiratory distress syndrome: Protective ventilation. *Arch Surg* 135: 126–135, 2000.
6. Sethi JM, Siegel MD: Mechanical ventilation in chronic obstructive lung disease. *Clin Chest Med* 21: 799–818, 2000.
7. Plant PK, Elliott MW: Chronic obstructive pulmonary disease * 9: Management of ventilatory failure in COPD. *Thorax* 58: 537–542, 2003.
8. Soto FJ, Varkey B: Evidence-based approach to acute exacerbations of COPD. *Curr Opin Pulm Med* 9: 117–124, 2003.
9. Davidson AC: The pulmonary physician in critical care. 11: Critical care management of respiratory failure resulting from COPD. *Thorax* 57: 1079–1084, 2002.
10. Mannino DM: COPD: Epidemiology, prevalence, morbidity and mortality, and disease heterogeneity. *Chest* 121: 121S–126S, 2002.
11. Nevins ML, Epstein SK: Predictors of outcome for patients with COPD requiring invasive mechanical ventilation. *Chest* 119: 1840–1849, 2001.
12. Nevins ML, Epstein SK: Weaning from prolonged mechanical ventilation. *Clin Chest Med* 22: 13–33, 2001.
13. Seneff MG, Wagner DP, Wagner RP, *et al*: Hospital and 1-year survival of patients admitted to intensive care units with acute exacerbation of chronic obstructive pulmonary disease. *JAMA* 274: 1852–1857, 1995.
14. Marcolin R, Mascheroni D, Pesenti A, *et al*: Ventilatory impact of partial extracorporeal CO2 removal (PECOR) in ARF patients. *ASAIO Trans* 32: 508–510, 1986.
15. Kolobow T, Gattinoni L, Tomlinson TA, Pierce JE: Control of breathing using an extracorporeal membrane lung. *Anesthesiology* 46: 138–141, 1977.
16. Kolobow T, Gattinoni L, Tomlinson T, *et al*: The carbon dioxide membrane lung (CDML): A new concept. *Trans Am Soc Artif Intern Organs* 23: 17–21, 1977.
17. Kolobow T, Gattinoni L, Fumagalli R, *et al*: Carbon dioxide and the membrane artificial lung: Their roles in the prevention and treatment of respiratory failure. *Trans Am Soc Artif Intern Organs* 28: 20–23, 1982.
18. Gattinoni L, Kolobow T, Damia G, *et al*: Extracorporeal carbon dioxide removal (ECCO2R): A new form of respiratory assistance. *Int J Artif Organs* 2: 183–185, 1979.
19. Gattinoni L, Kolobow T, Agostoni A, *et al*: Clinical application of low frequency positive pressure ventilation with extracorporeal CO2 removal (LFPPV-ECCO2R) in treatment of adult respiratory distress syndrome (ARDS). *Int J Artif Organs* 2: 282–283, 1979.
20. Gattinoni L, Agostoni A, Pesenti A, *et al*: Treatment of acute respiratory failure with low-frequency positive-pressure ventilation and extracorporeal removal of CO2. *Lancet* 2: 292–294, 1980.
21. Wang D, Lick S, Alpard SK, *et al*: Toward ambulatory arteriovenous CO2 removal: initial studies and prototype development. *ASAIO J* 49: 564–567, 2003.
22. Zwischenberger JB, Conrad SA, Alpard SK, *et al*: Percutaneous extracorporeal arteriovenous CO2 removal for severe respiratory failure. *Ann Thorac Surg* 68: 181–187, 1999.
23. Zwischenberger JB, Alpard SK, Tao W, *et al*: Percutaneous extracorporeal arteriovenous carbon dioxide removal improves survival in respiratory distress syndrome: A prospective randomized outcomes study in adult sheep. *J Thorac Cardiovasc Surg* 121: 542–551, 2001.
24. Conrad SA, Zwischenberger JB, Grier LR, *et al*: Total extracorporeal arteriovenous carbon dioxide removal in acute respiratory failure: a phase I clinical study. *Intensive Care Med* 27: 1340–1351, 2001.
25. Zwischenberger JB, Nguyen TT, Upp Jr. JR, *et al*: Complications of neonatal extracorporeal membrane oxygenation. Collective experience from the Extracorporeal Life Support Organization. *J Thorac Cardiovasc Surg* 107: 838–848; discussion 848-839, 1994.
26. Gaylor JD, Murphy JF, Caprini JA, *et al*: Gas transfer and thrombogenesis in an annular membrane oxygenator with active blood mixing. *Trans Am Soc Artif Intern Organs* 19: 516–524, 1973.
27. Hill JD, Iatridis A, O'Keefe R, Kitrilakis S: Technique for achieving high gas exchange rates in membrane oxygenation. *Trans Am Soc Artif Intern Organs* 20A: 249–252, 1974.
28. Lewis FR, Tylke JA, Winchell HS: A combined membrane pump-oxygenator: Design and testing. *Trans Am Soc Artif Intern Organs* 20A: 253–260, 1974.
29. Astolfi D, Christlieb I: [Artificial heart-lung: method of its preparation and assembling. I. Disk oxygenator (Kay-Cross) machines]. *Cir Ginecol Urol* 19: 218–224, 1965.
30. Dietmann K, Kreutzberg B, Raschke E, Bernhard A: [Construction principles and mechanism of action of a rotating disk oxygenator.]. *Thoraxchirurgie* 9: 516–529, 1962.
31. Gille JP, Saunier C, Pham QT, *et al*: [Extracorporeal purification of carbon dioxide: efficiency of a disk oxygenator during experimental hypercapnia]. *Pathol Biol (Paris)* 17: 371–377, 1969.
32. Makarewicz AJ, Mockros LF, Anderson RW: A pumping artificial lung. *ASAIO J* 40: M518–M521, 1994.
33. Makarewicz AJ, Mockros LF, Mavroudis C: New design for a pumping artificial lung. *ASAIO J* 42: M615–619, 1996.
34. 7199-1996 AAI: *Cardiovascular Implants and Artificial Organs: Blood-Gas Exchangers.* Association for the Advancement of Medical Instrumentation, 1997.
35. Hewitt TJ, Hattler BG, Federspiel WJ: A mathematical model of gas exchange in an intravenous membrane oxygenator. *Ann Biomed Eng* 26: 166–178, 1998.
36. Perry RH GD, Maloney JO (ed): *Perry's Chemical Engineers' Handbook.* New York, McGraw-Hill Companies, 1997.
37. Golob JF, Federspiel WJ, Merrill TL, *et al*: Acute in vivo testing of an intravascular respiratory support catheter. *ASAIO J* 47: 432–437, 2001.
38. KollerT Jr, Hawrylenko A: Contribution to the in vitro testing of pumps for extracorporeal circulation. *J Thorac Cardiovasc Surg* 54: 22–29, 1967.
39. Medtronic I: Medtronic Carmeda Affinity NT Oxygenator. *Product Literature*, 2001.
40. Leverett LB, Hellums JD, Alfrey CP, Lynch EC: Red blood cell damage by shear stress. *Biophys J* 12: 257–273, 1972.
41. Cooney DO (ed): *Biomedical Engineering Principles: An Introduction to Fluid, Heat and Mass Transport Processes.* New York, NY, Marcel Dekker, Inc., 1976.
42. Yu SC, Ng BT, Chan WK, Chua LP: The flow patterns within the impeller passages of a centrifugal blood pump model. *Med Eng Phys* 22: 381–393, 2000.
43. Song X, Throckmorton AL, Wood HG, *et al*: Computational fluid dynamics prediction of blood damage in a centrifugal pump. *Artif Organs* 27: 938–941, 2003.
44. Burgreen GW, Antaki JF, Wu ZJ, Holmes AJ: Computational fluid dynamics as a development tool for rotary blood pumps. *Artif Organs* 25: 336–340, 2001.
45. Asztalos B, Yamane T, Nishida M: Flow visualization analysis for evaluation of shear and recirculation in a new closed-type, monopivot centrifugal blood pump. *Artif Organs* 23: 939–946, 1999.
46. Apel J, Paul R, Klaus S, *et al*: Assessment of hemolysis related

quantities in a microaxial blood pump by computational fluid dynamics. *Artif Organs* 25: 341–347, 2001.
47. Apel J, Neudel F, Reul H: Computational fluid dynamics and experimental validation of a microaxial blood pump. *ASAIO J* 47: 552–558, 2001.
48. Anderson JB, Wood HG, Allaire PE, *et al*: Computational flow study of the continuous flow ventricular assist device, prototype number 3 blood pump. *Artif Organs* 24: 377–385, 2000.
49. Tsukiya T, Taenaka Y, Tatsumi E, Takano H: Performance of a newly developed implantable centrifugal blood pump. *ASAIO J* 47: 559–562, 2001.
50. Sekine K, Mitamura Y, Murabayashi S, *et al*: Development of a magnetic fluid shaft seal for an axial-flow blood pump. *Artif Organs* 27: 892–896, 2003.
51. Vranckx P, Foley DP, de Feijter PJ, *et al*: Clinical introduction of the Tandemheart, a percutaneous left ventricular assist device, for circulatory support during high-risk percutaneous coronary intervention. *Int J Cardiovasc Intervent* 5: 35–39, 2003.
52. Takami Y, Makinouchi K, Otsuka G, Nose Y: Quantitative approach to control spinning stability of the impeller in the pivot bearing-supported centrifugal pump. *Artif Organs* 21: 1292–1296, 1997.